CONTENTS

MINIREVIEWS

COMMUNICATIONS

Ylides

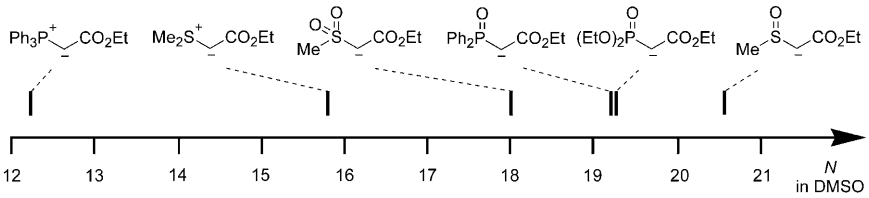

The nucleophilicity parameters of stabilized sulfur ylides, methylsulfonyl-, and methylsulfinyl stabilized carbanions have been determined from the rates of their reactions with benzhydrylium ions and quinone methides. Direct comparisons of the nucleophilic reactivities of sulfur and phosphorus ylides as well as their related carbanions have now become possible.

Coordination Complexes

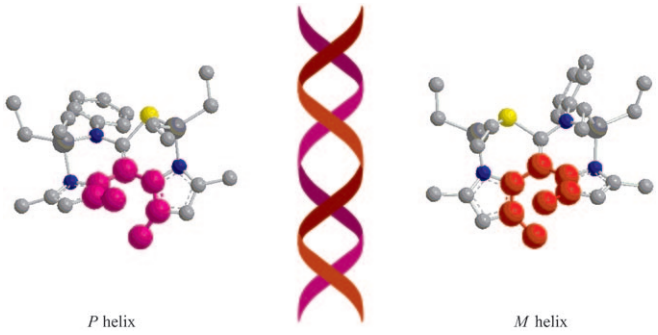

In a twist: The synthesis of novel architectures, through the use of versatile heteroscorpionate ligands, was developed that allows helical chirality in aluminium complexes (see figure).

Solar Cells

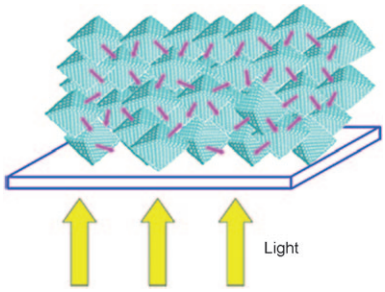

Hierarchical SnO_2 octahedra consisting of SnO_2 nanoparticles ($\approx$30 nm in diameter) can be successfully fabricated by a fast sonochemical process followed by heat treatment (see figure). The dye-sensitized solar cell based on the photoelectrodes consisting of the bifunctional hierarchical octahedral SnO_2 shows a power conversion efficiency of 6.40%.

Helical Superstructures

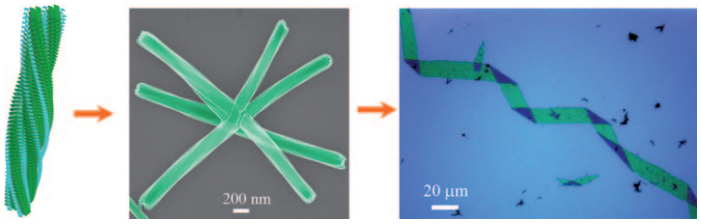

Tuning hierarchical superstructures of helical nanofibers: Helical conducting polyaniline (PANI) nanofibers can self-assemble into linear nanofibers, branched nanofibers, and microribbons by controlling their aggregation processes. Structural studies indicated that helical PANI molecules are arranged normal to the long axis of nanofibers, which is very similar to the arrangement of peptides in β sheets (see figure).

CONTENTS

Borate: guilty and charged! The borate ion, and possibly carbonate, enhances rates of steady oxygen-isotope exchanges at some, but not all, structural sites in polyoxometalate ions. Addition of an oxygen atom to an incoming neutral boric acid molecule (blue = boron) from a bridging oxygen atom on a decametalate ion is shown here.

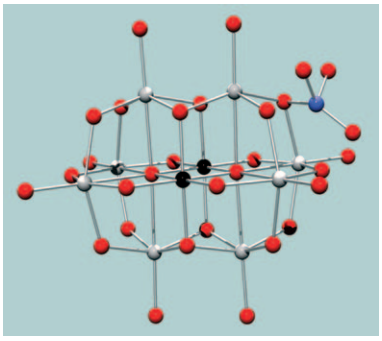

A pocket of resistance: We have analysed the molecular determinants for nucleotide recognition by the resistance enzyme ANT(4′). Our results demonstrate that its binding epitope is restricted to the inorganic triphosphate fragment. Strikingly, this, together with longer polyphosphate oligomers, can be employed as cosubstrates in aminoglycoside inactivation (see figure), implying a change in the normal activity of the enzyme. These results have implications in the design of specific enzymatic inhibitors.

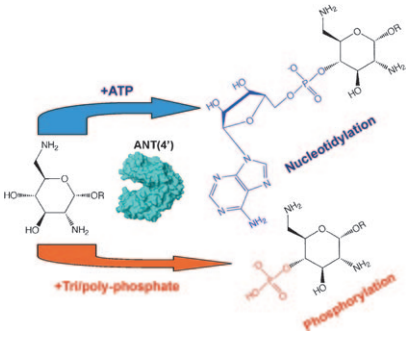

Smart release on demand: A general pH-responsive supramolecular nanovalve operating in aqueous media has been designed by using mesoporous organosilica hollow nanospheres as nanocontainers (see picture). The nanovalve is capable of storing guest molecules within the hollow core and mesopore shell and releasing them on demand by acid/base triggering of the capping molecule, demonstrating a delicate vehicle for controlled release.

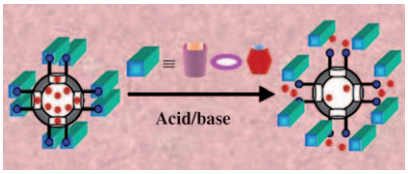

Bionanoprobes with high dispersion stability in water, excellent photostability, and biocompatibility were prepared by encapsulating [Eu(tta)$_3$dpbt] (tta = thenoyltrifluoroacetonato, dpbt = 2-(*N*,*N*-diethylanilin-4-yl)-4,6-bis-(3,5-dimethylpyrazol-1-yl)-1,3,5-triazine) in water-dispersible poly(methyl methacrylate-*co*-methacrylic acid) nanospheres and modifying the nanosphere surfaces with a monoclonal antibody (see scheme). The bionanoprobes exhibited excellent performance in the target-specific imaging of live cancer cells.

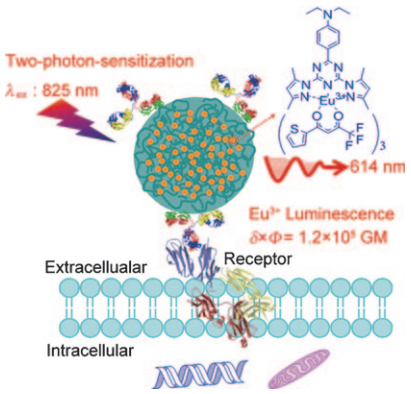

FULL PAPERS

Supramolecular Assembly

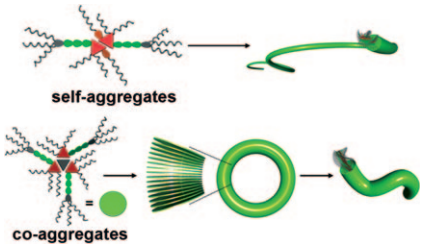

Line up! Oligo(*p*-phenylenevinylene)s capped on one end by a monotopic melamine hydrogen-bonding module can self- and co-aggregate with cyanuric acid to produce various self-assembled architectures (see figure).

Polymerization

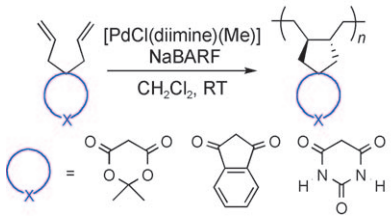

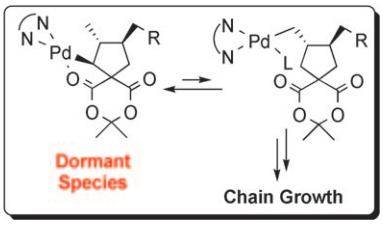

Pd complexes with diimine ligands catalyze the cyclopolymerization of functionalized 1,6-heptadienes (see scheme), as well as their copolymerization with ethylene and 1-hexene. The resultant polymers contain 1,2-*trans*-fused cyclopentane rings along the polymer chain.

Radical Reactions

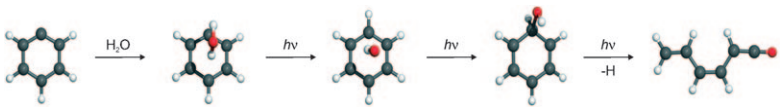

The phenyl radical forms a hydrogen-bonded complex with water that could be isolated in solid argon at 10 K. Visible-light irradiation results in the transfer of a hydrogen atom from water to the phenyl radical under formation of a complex between OH and benzene. Prolonged irradiation results in the complete destruction of the benzene molecule and formation of a ring-opened ketene (see scheme).

Organogels

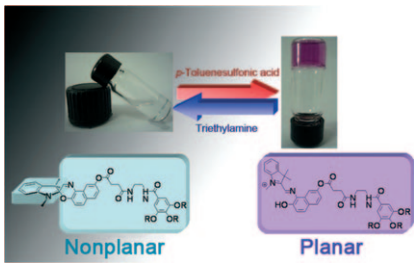

I like the way you move: A series of photochromic spironaphthoxazine derivatives has been designed, synthesized, and characterized by using ^{1}H NMR spectroscopy, FAB mass spectrometry, and elemental analysis. The photophysical and photochromic behavior has also been investigated. Two of the compounds have been shown to be capable of forming stable thermoreversible organogels in organic solvents (see figure).

CONTENTS

In a new light: Polyelectrolyte (sodium poly(styrenesulfonate) (NaPSS)) complexation followed by polyelectrolyte-assisted nanoparticle formation induces fluorescence enhancement by nearly two orders of magnitude (see picture) in a quinodimethane-based molecule (7,7-bis(piperazinium)-8,8-dicyanoquinodimethane bis(*p*-toluenesulfonate) (BT_2)).

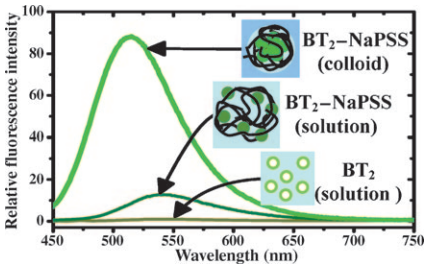

Mixed borohydrides: The synthesis, structure determination and decomposition pathway of a new complex double-cation borohydride with a very high hydrogen density are presented. The unique 3D-framework structure (see figure) contains complex anions $[Al(BH_4)_4]^-$ and cations $[Li_4(BH_4)]^{3+}$, which rationalise the unexpected stoichiometry $Al_3Li_4(BH_4)_{13}$.

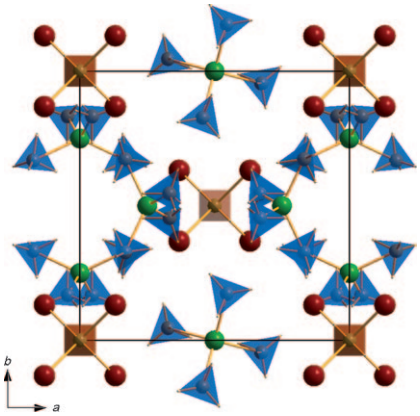

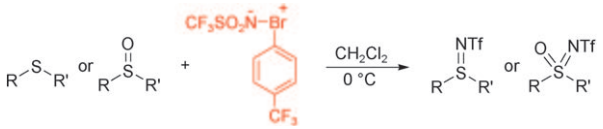

Metal-free imination: Exposure of sulfides and sulfoxides to triflylimino-λ^3-bromane in CH_2Cl_2 at 0 °C results in a facile transfer of the sulfonylimino group to sulfur atoms and affords *N*-triflylsulfilimines and -sulfoximines in high yields, under transition-metal-free conditions (see scheme).

Solid-solution photocatalyst: A hierarchical macro-/mesoporous (HMM) $Ce_{0.49}Zr_{0.37}Bi_{0.14}O_{1.93}$ solid-solution network (see picture) has been fabricated by a polymerization–carbonization–oxidation route. The obtained material combines high specific surface area, HMM structure, and high crystallinity, and as a result shows a strong structure-induced enhancement of visible-light harvest and enhanced visible-light photocatalytic activity in the photodegradation of methyl orange.

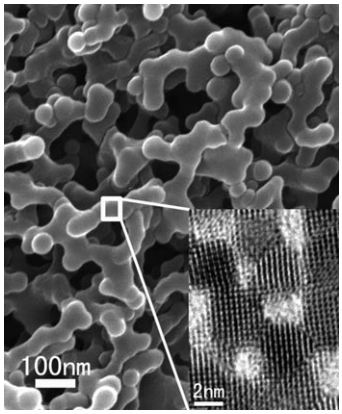

Metathesis

Latent catalysts: New ruthenium bidentate benzylidene catalysts based on sulfur and nitrogen chelation are presented (see figure). The catalysts were thoroughly characterised and studied by spectroscopic and crystallographic techniques, and their reactivity in several metathesis reactions is described and analysed.

Nucleophilic Addition

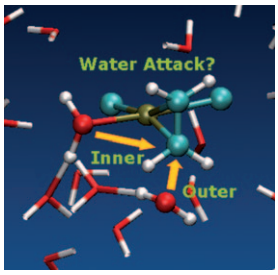

Wacker job: Does the nucleophilic addition step of the Wacker process proceed through an inner- or an outer-sphere mechanism (see image)? Ab initio molecular dynamics indicate that the outer-sphere mechanism is the less-energy-demanding pathway.

Supramolecular Chemistry

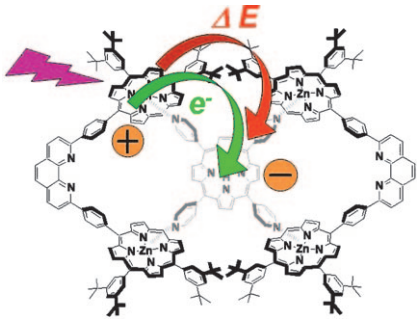

Something a little unusual: A surprising electron transfer from a zinc porphyrin to a free-base porphyrin is detected in a noncovalent pentaporphyrin array (see figure).

Zinc Oxide

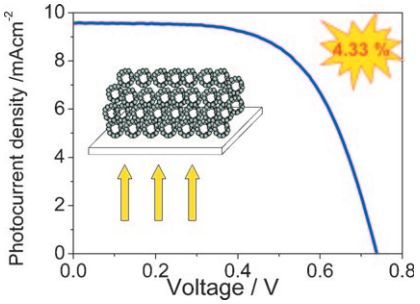

More efficient power conversion: Hierarchical ZnO hollow spheres (400–500 nm in diameter) consisting of ZnO nanoparticles with a diameter of approximately 15 nm have been successfully prepared by a facile and rapid sonochemical process. The power conversion efficiency of the dye-sensitized solar cells based on hierarchical ZnO hollow spheres is 4.33 %, which represents a 38.8 % increase compared to that of a ZnO nanoparticle photoelectrode (3.12 %).

Molecular Magnetism

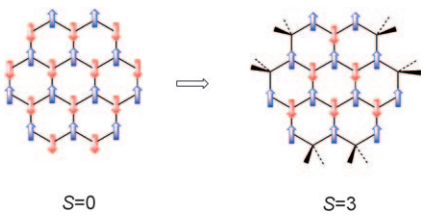

Smart saturation: Saturating properly chosen vertices of polycyclic conjugated hydrocarbons may lead to high-spin organic units (see figure).

Dye classification: Based on the results of quantum-chemical and spectral investigations of trimethine cyanine dye derivatives of 2-azaazulene, we propose a new classification of the terminal heterocycles (traditional Brooker's type and Azaazulene-like residues), and thus three types of cyanine dyes: Brooker's cyanines (BC), azaazulene-like (AAz) cyanines, and mixed AAz-BC dyes bearing the terminal groups of both types (see figure).

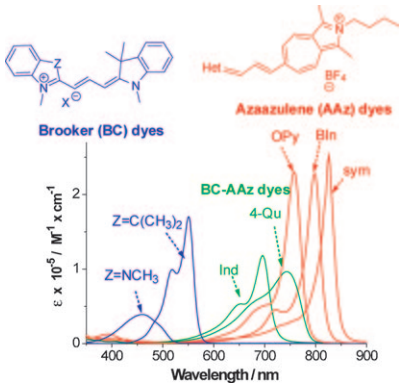

Electron Transitions

Three out of five members of the $Fe(X\text{-}py)_2[Ag(CN)_2]_2$ (py = pyridine; X = H, 3-Cl, 3-Me, 4-Me, 3,4-Me_2) family of 2D polymeric spin-crossover (SCO) compounds (see picture) are among the rare examples of non-binuclear SCO compounds that show two-step behaviour not only in the thermal spin transition, but also in the relaxation of the photoinduced high-spin metastable state, as revealed by magnetic and calorimetric measurements.

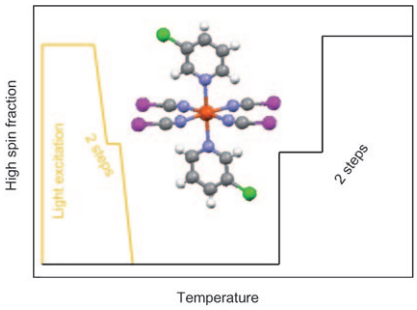

Spin-Crossover Compounds

Magnetic helicates: Enantiomerically pure trinuclear helicate-type complexes are self-assembled in a hierarchical process. With paramagnetic metal ions they show some interesting magnetic behavior (see figure).

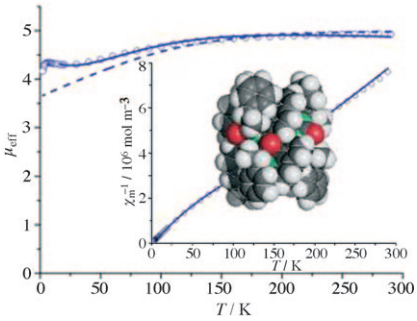

Self-Assembly

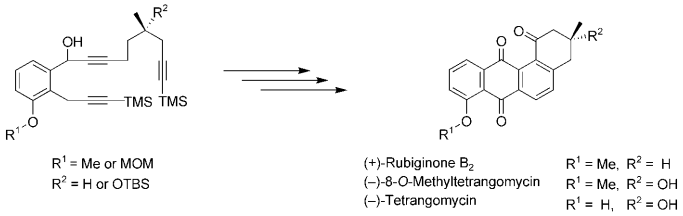

Like, totally: A convergent and asymmetric total synthesis of naturally occurring angucyclinone antibiotics (+)-rubiginone B_2, (−)-tetrangomycin, and (−)-8-*O*-methyltetrangomycin by means of intramolecular cobalt-mediated [2+2+2] cycloaddition was established (see scheme).

Antibiotics

Azo Compounds

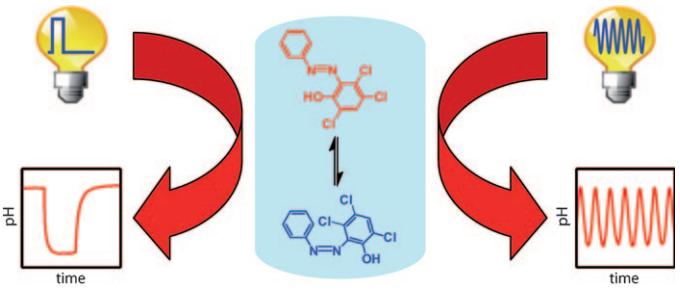

Sink or swing: The *trans*-to-*cis* isomerization of 2-hydroxyazobenzenes under UV light results in a tunable transient change of the protonation constant. Up to 2 pH units of fast, reversible pH drops and pH oscillations have been generated by shaping single-wavelength illumination (see picture).

Energy Transfer

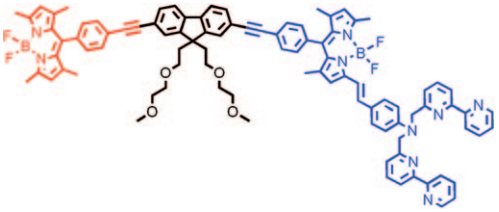

Energy exchange: Intercomponent photoinduced energy transfer takes place between different 4,4-difluoro-4-bora-3a,4a-diaza-*s*-indacene (Bodipy) subunits separated by a fluorene spacer (see figure). The efficiency and rate of such a process can be tuned by the presence of protons.

Group 13 Elements

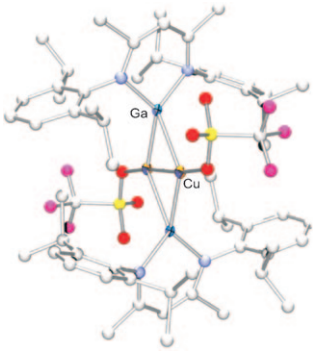

[{(ddp)GaCu(OTf)}$_2$]

Right system? Reactions of suitable copper precursors with gallium(I) species lead to three dinuclear copper complexes with direct Cu–Ga donor–acceptor interactions. Depending on the ligand system and the oxidation state, complexes with very short Cu···Cu distances and also the first complex of Cu^0 are formed (see picture).

Main Group Chemistry

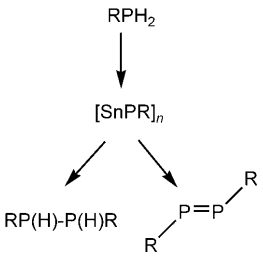

Release me: Tin(II) phosphanediides are readily prepared by deprotonation of RPH_2 with $Sn(NMe_2)_2$ at room temperature. These species exhibit interesting thermolysis reactions, giving rise to diphosphanes, diphosphenes and tin metal on heating (see scheme).

CONTENTS

Cycloaddition and Cycloreversion

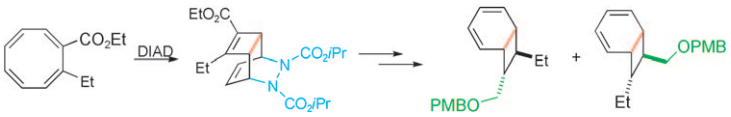

Toss diazo into the ring! [4+2] Cycloaddition reactions between 1,8-disubstituted cyclooctatetraenes and diazo compounds provide either 2,3- or 3,4-disubstituted adducts. Product distribution can be controlled by modulating the dienophile or the electron density of the cyclooctatetraene. The adducts displayed selective action against various human tumour cell types, whilst also forming the basis of a new pathway to the synthetically challenging bicyclo[4.2.0]octa-2,4-diene family (see scheme).

Trienol Ethers

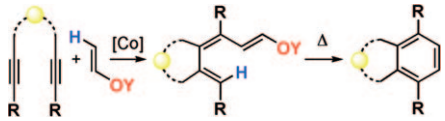

Competing pathways: Trienol ethers, including diborylated derivatives, are constructed by cobalt-mediated linear co-oligomerization of alkynes with enol ethers. This formal alkyne coupling/C–H activation sequence proceeds in a highly regio- and diastereoselective fashion. Thermal electrocyclic ring closure, coupled with dehydroalkoxylation, leads to arene derivatives (see figure), the sequence constituting a formal [2+2+2] cycloaddition of alkynes to acetylene.

Bioorganometallic Chemistry

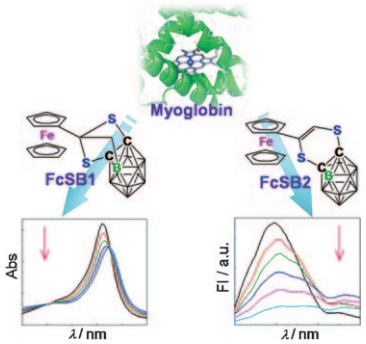

Go bio! Two ferrocene-substituted dithio-*o*-carborane isomers (FcSB1 and FcSB2) show a different binding affinity to myoglobin and affect the spin state of the heme iron center and the conformation of aromatic fluorophores in the protein matrix. The exploration of such biointeractions provides insights into the promising bioapplications of the relevant multifunctional organometallic complexes.

* Author to whom correspondence should be addressed

Supporting information on the WWW (see article for access details).

VIP Full Papers labeled with this symbol have been judged by two referees as being "very important papers".

A video clip is available as Supporting Information on the WWW (see article for access details).

SERVICE

Issue 28/2010 was published online on July 19, 2010

CORRIGENDUM

Chem. Eur. J., **2010**, *16*

DOI: 10.1002/chem.201000076

In this article, reference [47] contains an incorrect author name and the wrong journal has been cited. The correct reference is given below. The authors apologize for this mistake.

[47] R. Lalor, J. L. DiGesso, A. Mueller, S. E. Matthews, *Chem. Commun.* **2007**, 4907–4909.

